Shahrood University of Technology
Iranian Society of Mining Engineering (IRSME)

Journal of Mining and Environment (JME)

journal homepage: www.jme.shahroodut.ac.ir

THOMSON REUTERS

Vol. 11, No. 1, 2020, 281-300.
DOI: 10.22044/jme.2019.9027.1790

Prediction of Blasting Cost in Limestone Mines Using Gene Expression Programming Model and Artificial Neural Networks

R. Bastami[1], A. Aghajani Bazzazi[2], H. Hamidian Shoormasti[3*], K. Ahangari[1]

1. Department of Mining Engineering, Faculty of Engineering, Science and Research Branch, Islamic Azad University, Tehran, Iran.
2. Department of Mining Engineering, Faculty of Engineering, University of Kashan, Kashan, Iran.
3. Department of Mining Engineering, Qaemshahr Branch, Islamic Azad University, Qaemshahr, Iran.

Received 13 October 2019; received in revised form 28 December 2019; accepted 29 December 2019

Keywords

Blasting cost

Limestone mines

Gene expression programming

Non-linear multivariate regression

Artificial neural networks

Modeling

Abstract

The use of blasting cost (BC) prediction to achieve optimal fragmentation is necessary in order to control the adverse consequences of blasting such as fly rock, ground vibration, and air blast in open-pit mines. In this research work, BC is predicted through collecting 146 blasting data from six limestone mines in Iran using the artificial neural networks (ANNs), gene expression programming (GEP), linear multivariate regression (LMR), and non-linear multivariate regression (NLMR) models. In all models, the ANFO value, number of detonators, Emolite value, hole number, hole length, hole diameter, burden, spacing, stemming, sub-drilling, specific gravity of rock, hardness, and uniaxial compressive strength are used as the input parameters. The ANN model results in the test stage indicating a higher correlation coefficient (0.954) and a lower root mean square error (973) compared to the other models. In addition, it has a better conformity with the real blasting costs in comparison with the other models. Although the ANNs method is regarded as one of the intelligent and powerful techniques in parameter prediction, its most important fault is its inability to provide mathematical equations for engineering operations. In contrast, the GEP model exhibits a reliable output by presenting a mathematical equation for BC prediction with a correlation coefficient of 0.933 and a root mean square error of 1088. Based on the sensitivity analysis, the spacing and ANFO values have the maximum and minimum effects on the BC function, respectively. The number of detonators, Emolite value, hole number, specific gravity, hardness, and rock uniaxial compressive strength have a positive correlation with BC, while the ANFO value, hole length, hole diameter, burden, spacing, stemming, and sub-drilling have a negative correlation with BC.

1. Introduction

The primary purpose of blasting is an optimal fragmentation and displacement of crushed rocks at the lowest cost. Some studies have indicated that only about 20-30% of all energies derived from explosives is spent on fragmentation and rock displacement, and the rest is wasted in the form of undesirable destructive phenomena such as ground vibration, air blast, fly rock, and back break [1]. These materials have caused many problems for the health of miners and locals, often resulting in litigation between the owner of the mine and local residents [2-4]. Evaluating the blasting cost (BC) without regarding the adverse consequences of blasting is meaningless. Given the remarkable importance and impact of blast on the cost of mineral extraction, it is necessary to provide a model to predict BC. Therefore, calculating the optimal BC to achieve an optimal fragmentation with respect to the blasting constraints is a major issue in the mining industry.

Corresponding author: hhamidian@qaemiau.ac.ir (H. Hamidian Shoormasti).

The most important studies on BC and the related issues are as what follows. Jimeno *et al*. [5] have presented the basic equation to calculate the cost of each drilling meter based on the direct and indirect costs. Direct costs include the personnel, maintenance, energy, grease, oil, rad, drill bit, etc., and indirect costs include insurance, tax, depreciation, and so on. Kanchibotla [6] has studied the maximum profitability, costs, and optimal blasting in an open-pit coal mine and a gold mine using the computer simulation models and field studies. Rajpot [7] has surveyed the impact of the fragmentation properties on BC and presented a model to evaluate the impact of hole diameter on the blasting requirements in order to achieve fragmentation d_{80} and calculate the blast design parameters for the particle size of 75-350 mm. Usman and Muhammad [8] have conducted a PCA-combined analysis on the parameters and data of 31 blasts in cement mines in the northern Pakistan; these parameters were utilized as a model for evaluating BC. In another study, Afum and Temeng [9] have surveyed the cost reduction of drilling and blasting in an open-pit gold mine in Ghana at three pits through blasting optimization and the use of the Kuz-Ram model. They could ultimately obtain an average of 25-56 cm fragmentation. Adebayo and Mutandwa [10] have studied the relationship between the blasting hole deviation, rock size, and fragmentation cost using ANFO, heavy ANFO, and emulsions in the holes with 191-311 mm diameter. The results obtained showed that the average rock size decreased by increasing the hole deviation, while the drilling and blasting costs increased. Ghanizadeh *et al*. [11] have presented BC per cubic meters as a linear model using the Comfar software as well as the statistical methods as a function of hole diameter, bench height, uniaxial compressive strength, and direction of joints. Miranda *et al*. [12] have used the numerical methods to find the minimum BC, compared to the traditional and experimental methods. This model is based on the development of blast patterns with the automatic adjustment of burden, spacing, stemming, sub-drilling, and number of holes in order to ensure the production demand in terms of the blast volume. Bakhshandeh *et al*. [13] have proposed a mathematical model for estimation of BC at the gypsum mine of Baghak. The input variables used were burden, spacing, hole diameter, stemming length, charge density, and charge weight. Finally, the non-linear model was optimized considering the constraints by the simulated annealing.

During the recent decades, the intelligence techniques such as the artificial neural networks (ANNs), fuzzy inference system (FIS), neuro-fuzzy inference system (ANFIS), and support vector machine (SVM) have been widely used in geosciences to predict the target parameters. Compared to the traditional methods, these techniques have significant features [14, 15]. Although they are regarded as powerful methods for parameter prediction, they do not provide the mathematical equation for engineering activities [16]. In a study using multivariate regression and ANNs, Alvarez *et al*. [17] have predicted the blasting-induced peak particle velocity and frequency of vibration in an open-pit mine. The R^2 values were obtained as 0.98 and 0.95 for the peak particle velocity and vibration frequency using the ANNs method, respectively, compared to 0.5 and 0.15 by the linear multivariate regression (LMR), which indicated the superiority of the ANNs model. In a study using back-propagation neural network, Trivedi *et al*. [18] have predicted the rate of fly rock in Indian limestone mines using ANNs after propagation, and indicated that the amount of charge per hole, depth of holes, burden, spacing, stemming, hole diameter, powder factor, rock quality designation (RQD), and compressive strength were the most influential parameters in the fly rock distance. Nguyen *et al*. [19] have predicted the blasting-induced ground vibration using the ANNs model, experimental methods, and 68 blasting data in an open-pit mine in Vietnam. In this study, five models with different numbers of neurons and different hidden layers were developed. Finally, the 1-5-8-10-2 ANNs model with three hidden layers (compared to the other four models) and experimental techniques with the 0.964 and 0.738 values for R^2 and RMSE, respectively, was introduced as the best model. Gene expression programming (GEP) is able to solve non-linear engineering problems, and can propose a formula to predict a particular output using the inputs related to its model. Canakci *et al*. [20] have used the GEP model to predict rock compressive and tensile strength, and found that the results of the GEP model were in good consistency with the measured values. Ahangari *et al*. [21] have compared the performance of the ANFIS and GEP methods in predicting the effect of tunneling on people's residence based on the data collected from 53 tunnels. They concluded that GEP was a superior model than ANFIS. Monjezi *et al*. [22] have introduced a modified version of the USBM empirical equation using a new input called water factor (WF). They suggested that this

modified equation was more accurate than the other empirical equations. In addition, they used three predictive models, namely LMR, non-linear multivariate regressions (NLMR), and GEP. Finally, the GEP model with the 0.918 and 2.223 values for R^2 and RMSE, respectively, was introduced as the best model. Dehgani [23] has used GEP to predict the variations in copper price. The results obtained were compared with those of the other classical methods. It was revealed that GEP was more accurate than the time series and multivariate regression methods.

Most of the above studies have been conducted on determining the relationship between BC and minerals' transportation cost, reducing the drilling and blasting costs, investigating the impact of fragmentation properties on BC, and presenting a BC model in a particular mine and the adverse consequences of blasting. Given that blasting is the first step in the production process in open-pit mines and the cost of this step is 8-12% of the total mining costs [8], and lack of any study in the literature in predicting BC in most minerals including limestones, it is necessary to provide a model for this purpose. In the present work, the GEP, ANN, NLMR, and LMR models were used to predict BC in limestone mines, and the results obtained were compared with the real data collected from six limestone mines in Iran.

2. Methodology

The following measures were taken for BC prediction (Figure 1):

- Data collection and determination of the input, output, and constraints parameters;
- BC modeling using the GEP, ANN, NLMR, and LMR methods;
- Comparing the performance of models with each other and selecting the best model as the research output.

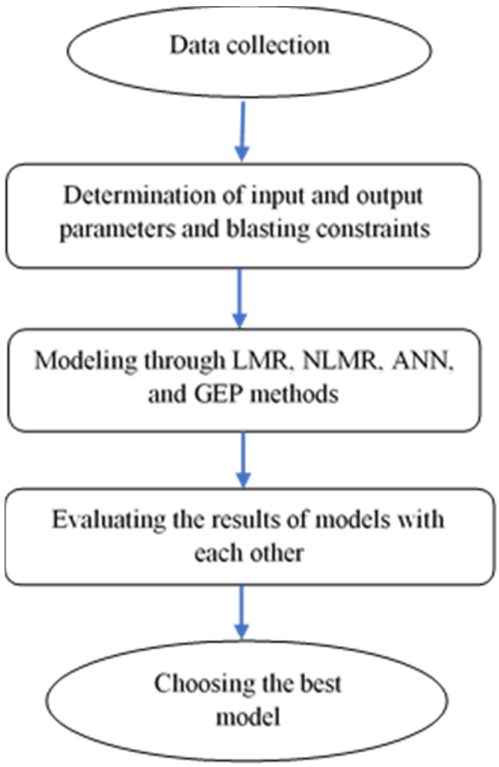

Figure 1. Steps of BC prediction.

2.1. Gene expression programming (GEP)

GEP has been extracted from Genetic Algorithm (GA) and Genetic Programming (GP), which was invented by Ferreira in 1999 [24]. In this method, the linear and simple chromosomes of constant length, similar to the GA and branch structures of different sizes and shapes, are combined with decomposing trees in GP, known as Expression Tree (ET) [25, 26].

In GEP, different phenomena are modeled using a set of functions and terminals. The set of terminals consists of constant values and independent variables of the problem [24, 27-32]. Here, a chromosome includes a coded linear sequence of

fixed length, which can be a combination of one or more genes [33].
The genes consist of two parts: head and tail. The head section can include functions and terminals, while the tail can only contain terminals. The codes for each gene result in the formation of a sub-ET, and the sub-ETs interact to form a larger and more complex ET. In order to form this complex structure, the sub-ETs are linked together by a function called the linking function [24, 34]. In the GEP algorithm, the mutation, inversion, transposition, and insertion sequence elements, and recombination are applied to the chromosomes orderly [24-26, 34-37]. A flowchart of the GEP algorithm is schematically shown in Figure 2.

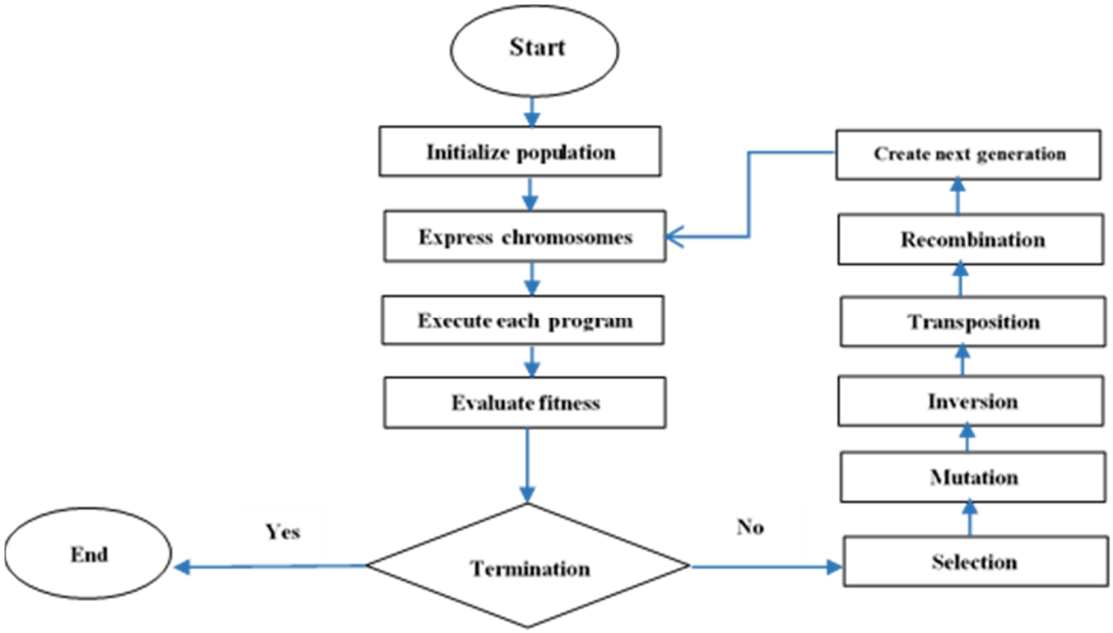

Figure 2. Flowchart of the GEP algorithm [38].

2.2. Artificial neural networks (ANNs)

The neural network (NN) is actually an imitation of the human brain [39]. Modeling with this network involves the structure design, and determining an appropriate train law and transfer function. In the present work, the network used was a multi-layer perceptron (MLP), each layer consisting of a matrix and bias vector and an output vector [40, 41]. There are several techniques in the MLP training process; however, the feed-forward back-propagation algorithm has more advantages over the other methods. Each input is weighted with an appropriate weighting factor (w). These weights are first assigned randomly. Then the network is modified during the learning process by reducing the error rate, and finally, its final values are determined [42-44].
There are basically three types of layers in NNs: an input layer, one or more middle layers, and an output layer. The number of neurons in the input and output layers is determined based on the number of input and output parameters and the number of middle layers along with the number of neurons in each layer with respect to the complexity of the problem by trial-and-error [45-47].
Different transfer functions can be used to create the desired output. Hardlims, Purelin, Poslin, Tansig, and Logsig are among these functions. The model accuracy is determined by comparing the ANNs and actual outputs [48].

3. Database and statistical analysis

In this research work, the data from six limestone mines in Iran was collected to predict and validate the GEP and ANN models. Table 1 shows the geographical coordinates and specifications of these mines.
In order to obtain the real data, the BC data of six limestone mines from 2011 to November 2018 was collected. Then the data was updated according to the price of explosives and BCs of January 2019, and became the basis of the research work. Based on the data, Figure 3 illustrates the components of the average BC as percentage. Figure 4 shows the geographical location of limestone mines. Table 2 displays the input, output, constraints, and statistical properties of these parameters.

Table 1. Geographical coordinates and specifications of the studied mines (source: http://ime.org.ir).

Row	Name of mine	Proven reserve (ton)	Annual extraction capacity	Geographical coordinates (WGS 84)		
				Nearest city	Latitude	Longitude
1	Abelou	89340000	4000000	Neka	36° 38' 5"	53° 21' 3"
2	Tajareh	4300000	150000	Khorramabad	33° 30' 5"	48° 29' 44"
3	Moslem Abad	7000000	300000	Hamedan	34° 39' 37"	48° 54' 22"
4	Tang Fani	900000	100000	Pol Dokhtar	33° 1' 24"	47° 46' 43"
5	Sepahan Mobarakeh	13500000	600000	Esfahan	32° 26' 28.37"	51° 28' 4.63"
6	Barkhordar1	1600000	160000	Nurabad	34° 3' 8"	48° 12' 53"

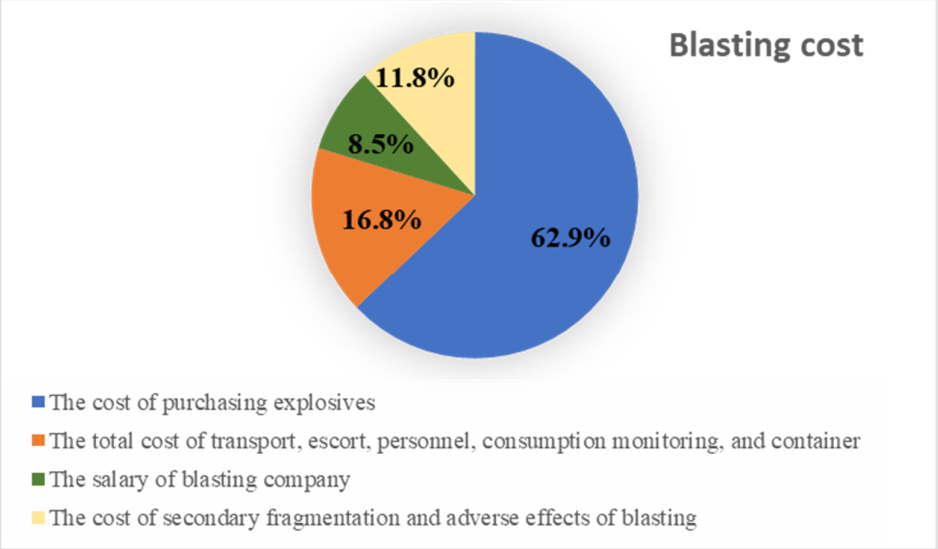

Figure 3. Components of BC.

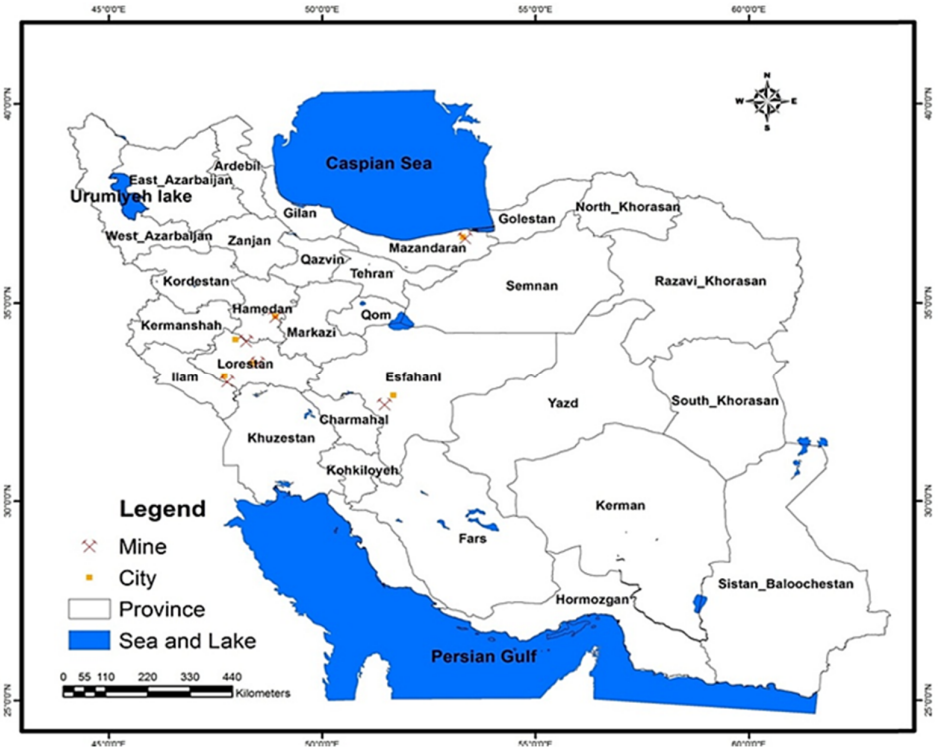

Figure 4. Geographical location of limestone mines.

Table 2. Input and output variables and their constraints.

Type	Parameter	Unit	Symbol	Max	Min	Mean	Standard deviation
Input	ANFO	2598.488	8551.3	1020	12400	AN	Kg
	Number of electric detonators	122.4	348	45	650	Det	-
	Emolite	115.4	295.4	40	600	EM	Kg
	Hole number	136.6	271.5	29	553	N	-
	Hole length	3.2	9.5	4	20.5	H	m
	Hole diameter	8.2	83	76	100	D	mm
	Burden	0.53	2.36	1.7	3.5	B	m
	Spacing	0.61	2.8	1.9	4	S	m
	Stemming	0.53	1.83	0.85	3.6	T	m
	Sub-drilling	0.42	0.82	0.2	1.5	J	m
	Specific gravity	0.04	2.66	2.6	2.7	Υr	ton/m^3
	Rock hardness	0.16	3.27	3	3.5	HA	Mhos
	Uniaxial compressive strength	49.9	600.6	530	671	σ_c	Kg/cm^2
Constraints	Fragmentation	7.94	36	20	47	Fr	cm
	Fly rock	19.2	97	60	140	Fl	m
	Back break	1.4	3.4	1	6	BB	m
Output	Blast cost	3995	13468	7157	23481	BC	Rials/ton

Using the box plot in the SPSS 24 software, the outlier data was identified and removed from the collected data, and then the number of data reached 146 patterns. A laser-meter and a total station surveying camera were used to measure the back-break and fly rock, respectively. The rock fragmentation resulting from each blasting pattern in the mine was measured using the Split Desktop V. 5 software. Imaging was randomly done with the help of a camera by considering the dimensional variability and using two scales at the top and bottom of the blasting coupe. The photographs were taken in large, medium, and small sizes. An average of 12-24 images was analyzed to eliminate the possible errors and increase the reliability of image analysis results in each blast of the studied mines. Then the images were analyzed using the Split Desktop 5 software to determine the real fragmentation (d_{80}). Next, the dimensional distribution curve of each blasting was obtained separately. Finally, the results of the analysis of all images in the software were combined. Figure 5 illustrates the steps of image analysis using the Split Desktop software in one of the studied mines.

The correlation between the input variables was obtained by the Pearson's correlation coefficient to predict BC based on the data collected from six limestone mines in the first stage (Table 3).

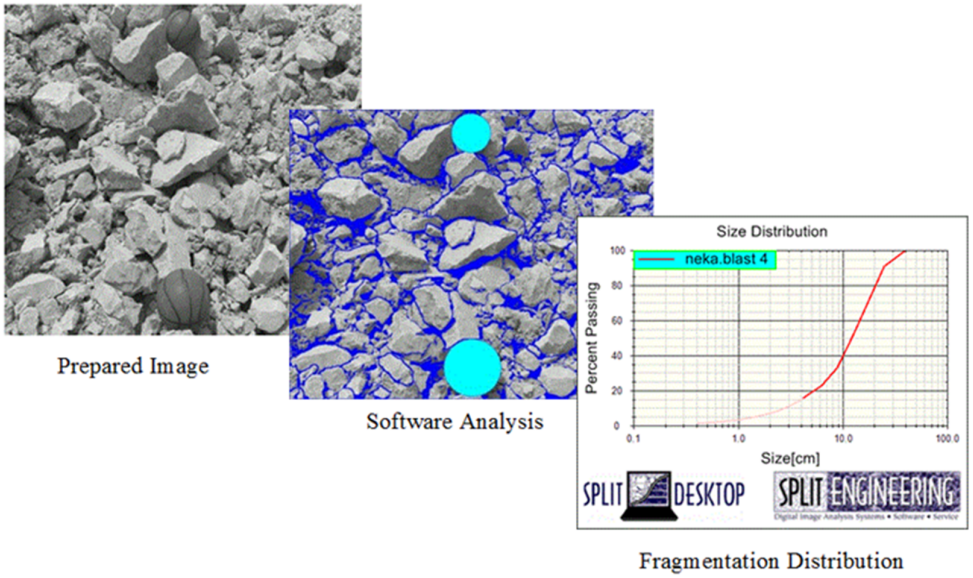

Figure 5. Process of using the Split Desktop software.

Table 3. Pearson's correlation coefficient matrix.

Variables	AN	Det	EM	N	H	D	B	S	T	J	γr	HA	σc
AN	1	0.554	0.567	0.34	0.295	0.206	-0.194	-0.254	-0.037	-0.031	0.424	0.376	0.194
Det	0.554	1	0.759	0.845	-0.394	-0.473	-0.59	-0.598	-0.559	-0.35	0.423	0.581	0.494
EM	0.567	0.759	1	0.699	-0.241	- 0.34	-0.518	-0.526	-0.431	-0.105	0.704	0.785	0.723
N	0.34	0.845	0.699	1	0.703	-0.681	-0.724	-0.711	-0.765	-0.542	0.294	0.579	0.51
H	0.295	-0.394	-0.241	0.703	1	0.675	0.569	0.535	0.757	0.579	0.061	-0.254	-0.27
D	0.206	-0.473	- 0.34	-0.681	0.675	1	0.631	0.514	0.647	0.47	-0.014	-0.249	-0.319
B	-0.194	- 0.59	-0.518	-0.724	0.569	0.631	1	0.964	0.802	0.747	-0.197	-0.544	-0.384
S	-0.254	-0.598	-0.526	-0.711	0.535	0.514	0.964	1	0.787	0.745	-0.217	-0.574	-0.391
T	-0.037	-0.559	-0.431	-0.765	0.757	0.647	0.802	0.787	1	0.769	-0.074	-0.47	-0.377
J	-0.031	- 0.35	-0.105	-0.542	0.579	0.47	0.747	0.745	0.769	1	0.398	0.07	0.114
γr	0.424	0.423	0.704	0.294	0.061	-0.014	-0.197	-0.217	-0.074	0.398	1	0.842	0.848
HA	0.376	0.581	0.785	0.579	-0.254	-0.249	-0.544	-0.574	-0.47	-0.07	0.842	1	0.945
σc	0.194	0.494	0.723	0.51	- 0.27	-0.319	-0.384	-0.391	-0.377	0.114	0.848	0.945	1

The rate of two-way linear relationship between the variables, known as the correlation matrix, is given in Table 3. In this matrix, the negative entries represent the inverse relation and the positive entries represent the direct relation between the variables.

4. BC prediction

4.1. Prediction with GEP model

This section aims to find a function in the template of *BC = f(AN, Det, EM, H, N, D, B, S, T, J,* ϒr, *HA, σc)* to predict BC, where AN, Det, EM, H, N, D, B, S, T, J, HA, ϒr, and σc are the independent variables and BC is the dependent variable.

Gene Xpro Tools is a powerful flexible modeling software developed by Ferreira *et al*. in 2000 and can be used for function finding, classification, time series prediction, and logic synthesis. In the present work, 80% of the data was used for modeling and 20% for random model testing out of the 146 blasts recorded in six limestone mines. Since the input and output parameters have different units and ranges of variation, the data must be normalized before any modeling in smart methods. Data normalization increases speed and decreases error in modeling and prevents over-fitting. In the present work, the data was normalized using Equation 1 at intervals 0 and 1:

$$X_{norm} = \frac{X_i - X_{\min}}{X_{\max} - X_{\min}} \quad (1)$$

where X_i indicates the initial data, X_{min} shows the minimum variable value, X_{max} is the maximum variable value, and X_{norm} is considered as the normalized value.

The modeling process can be described using the GEP algorithm in the following five steps [33, 49]:

A) Step 1: the cost function is determined to evaluate the fitness of the produced chromosomes. For this purpose, the root mean square error (RMSE) equation is used:

$$RMSE = \sqrt{\frac{1}{n}\sum_{i=1}^{n}(O_i - T_i)^2} \quad (2)$$

where O_i shows the i^{th} real value, T_i indicates the i^{th} predicted value, and n is considered as the number of data series.

B) Step 2: the terminals (problem inputs) and functions are defined to create the GEP chromosomes. In the present work, the terminals were 13 input parameters (Table 2), and the following important functions were selected by studying the structure of empirical relationships and examining the regression relationship between the inputs and outputs:

$$Functions\ Set = \{+, -, \times, \div, sqrt, Inv, \text{^}2, \text{^}3, \text{^}4, 3Rt, 4Rt, cos, tg, Not\} \quad (3)$$

where 3Rt and 4Rt are the third and fourth roots of the variable, respectively.

C) Step 3: the structure of the chromosomes must be determined. The structure of each chromosome depends on the number of genes and the size of their head. Increasing the number of genes and chromosomes can partly improve the performance of the GEP model. However, as the number of genes exceeds their optimal value, the complexity of the model increases, leading to a possible over-fitting phenomenon [33].

D) Step 4: genetic operators and their rates are determined. In the present work, all genetic operators were regarded as suggested by Ferreira and other researchers [22, 24, 36, 37and 50]. To determine the rate of operators, Ferreira proposes the values that are suitable for most of the engineering problems [24, 34]. Our investigations showed that the values proposed by Ferreira were appropriate for the present work.

E) Step 5: a linking function is required to bind the genes. In the present work, the addition linking function was used for a better performance. Table 4 displays the genetic operator rates and basic settings of the five models of the BC function.

Table 4. Genetic operator rates and basic settings of five BC function models.

Type of setting	Parameter	Value				
		1	2	3	4	5
Basic settings	Fitness function	RMSE	RMSE	RMSE	RMSE	RMSE
	Number of chromosomes	30	32	30	28	35
	Number of generations	9000	9000	9000	9000	9000
	Head size	9	12	10	10	8
	Number of genes	4	3	4	5	4
	Linking function	Addition	Addition	Addition	Addition	Addition
Genetic operators	Mutation rate	0.00138	0.00138	0.00138	0.00138	0.00138
	Inversion rate	0.00546	0.00546	0.00546	0.00546	0.00546
	IS transposition rate	0.00546	0.00546	0.00546	0.00546	0.00546
	RIS transposition rate	0.00546	0.00546	0.00546	0.00546	0.00546
	Gene transposition rate	0.00277	0.00277	0.00277	0.00277	0.00277
	One-point recombination rate	0.00277	0.00277	0.00277	0.00277	0.00277
	Two-point recombination rate	0.00277	0.00277	0.00277	0.00277	0.00277
	Gene recombination rate	0.00277	0.00277	0.00277	0.00277	0.00277

In the above steps, the adjusted GEP models were implemented and the values of the correlation coefficient (R^2) and RMSE were calculated for each one of the models in the train and test phases based on Equations 2 and 4 [38]. The results obtained are displayed in Table. 5.

$$R^2 = 100\left(\frac{\sum_{i=1}^{n}(T_i - \bar{T_i})\times(O_i - \bar{O_i})}{\sqrt{\sum_{i=1}^{n}(T_i - \bar{T_i})^2 \times \sum_{i=1}^{n}(O_i - \bar{O_i})^2}}\right)^2 \quad (4)$$

where O_i is the i[th] real value, T_i is the i[th] predicted value, $\bar{O_i}$ is the average real value, $\bar{T_i}$ is the average predicted value, and n is the number of series. Based on this table, model 3 was selected as the best GEP model with a higher accuracy and a lower error compared to the other models.

The superior chromosome has four genes in the BC function, each representing a sub-ET (Figure 6). A large tree is formed by joining these four sub-ETs by the addition function. Each one of the genes can be obtained from the corresponding mathematical equation (Equations. 5-8). Finally, the general relation of BC prediction using the GEP model is calculated by Equation 9.

Table 5. Evaluation criteria for five different GEP models.

Model No.	Training stage		Testing stage	
	R^2	RMSE	R^2	RMSE
1	0.919	1122	0.910	1356
2	0.904	1238	0.884	1435
3	0.943	961	0.933	1088
4	0.897	1269	0.864	1540
5	0.912	1172	0.913	1235

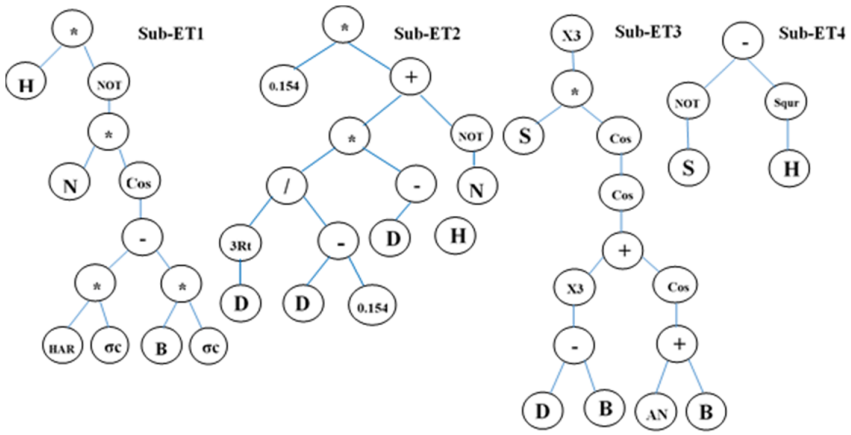

Figure 6. The tree structure of each gene in the GEP model for BC prediction.

$$sub-ET_1 : H' \times \left(1-\left(\mathrm{N}' \times \cos\left(HA' \times \sigma c' - B' \times \sigma c'\right)\right)\right) \quad (5)$$

$$sub-ET_2 : 0.154 \times \left(\frac{D'^{\left(\frac{1}{3}\right)}}{D'-0.154} \times \left(D'-H'\right)+1-\mathrm{N}'\right) \quad (6)$$

$$sub-ET_3 : \left(S' \times \cos\left(\cos\left(\left(D'-B'\right)^3+\cos\left(\mathrm{AN}'+B'\right)\right)\right)\right)^3 \quad (7)$$

$$sub-ET_4 : 1-S'-H'^{0.5} \quad (8)$$

$$BC = \left(Gene1+Gene2+Gene3+Gene4\right) \times 16324 + 7157 \quad (9)$$

The values of the decision variables $(\mathrm{AN}', \mathrm{N}', H', D', B', S', HA', \sigma c')$ of normal numbers are between zero and one in the models presented for the BC function, and the output indicates a natural value by applying the input coefficients and integers. Equations 10-17 should be used instead of the decision variables $(\mathrm{AN}', \mathrm{N}', H', D', B', S', HA', \sigma c')$ for the convenience of the user and for entering the natural numbers into the equations. Figure 7 indicates the relationship between the measured values of BC predicted with the help of the GEP model in the train phase:

$$\mathrm{AN}' = \frac{AN - 1020}{11380} \quad (10)$$

$$\mathrm{N}' = \frac{N - 29}{524} \quad (11)$$

$$H' = \frac{H - 3.99}{16.38} \quad (12)$$

$$D' = \frac{D - 76}{24} \quad (13)$$

$$S' = \frac{S - 1.9}{2.1} \quad (14)$$

$$HA' = \frac{HA - 3}{0.5} \quad (15)$$

$$B' = \frac{B - 1.7}{1.8} \quad (16)$$

$$\sigma c' = \frac{\sigma c - 530}{14} \quad (17)$$

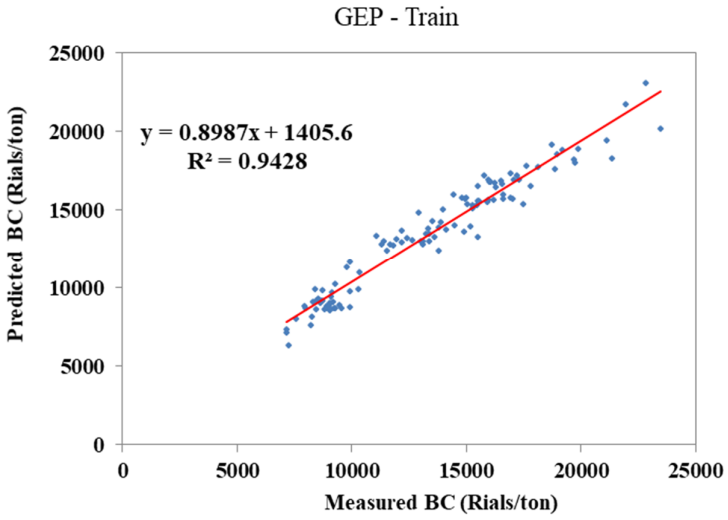

Figure 7. Relationship between the predicted and measured values of BC and GEP model (in the train phase).

4.2. Prediction with ANNs model

Selecting the number of datasets used to train network is very important. The lack or excess number of datasets used will decrease the performance of network. An optimal layout in each case is achieved by trial-and-error. In this research work, 146 data were randomly divided into the training (80%) and testing (20%) groups. The model was trained by the MLP method using the feed-forward back-propagation algorithm. The dataset was normalized to improve the efficiency of the train process with -1 to 1 values. Then different types of networks were tested with different layers and neurons as well as transferring functions in order to determine the optimal network structure with the least error [51]. R^2 and RMSE were determined for different network structures (Table 6).

As shown in Table 6, the MLP network (with feed forward, along with 13 input neurons, 14 neurons in the first middle layer, 5 neurons in the second middle layer, one output neuron, and the Logsig, Tansig, and Purlin transfer functions) is able to predict BC most accurately. This network with the architecture of 13-14-5-1 has the minimum estimation error, which is regarded as the appropriate model. Figure 8 displays the optimal network structure, and Figure 9 illustrates the relationship between the measured values of BC predicted with the ANNs model during the train phase. The appropriate network structure was determined by a form of test and error process. To this end, similar articles were studied; first, networks with one or two hidden layers were evaluated, which are often more suitable for the engineering problems [13, 46, 48].

In the GEP and regression models, two datasets (train and test) are used. Here, in order to compare the outputs of the ANN model with the actual data and the above-mentioned models, the validation and train data are classified into one category and the test data in another.

Table 6. R^2 and RMSE for some of the models.

No.	Architecture	Hidden activation	Output activation	All data	
				R^2	RMSE
1	13-15-1	Logsig	Purelin	0.954	853
2	13-20-1	Tansig	Purelin	0.963	775
3	13-12-1	Logsig	Poslin	0.477	4112
4	13-17-1	Tansig	Poslin	0.541	3994
5	13-17-5-1	Tansig-Tansig	Purelin	0.955	866
6	13-20-10-1	Logsig-Logsig	Purelin	0.945	942
7	13-6-18-1	Tansig-Tansig	Purelin	0.962	791
8	13-7-14-1	Logsig-Logsig	Purelin	0.955	870
9	13-16-8-1	Logsig-Logsig	Poslin	0.512	3995
10	13-22-12-1	Tansig-Tansig	Poslin	0.462	4033
11	13-14-5-1	Logsig-Tansig	Purelin	0.971	677
12	13-19-11-1	Tansig-Logsig	Purelin	0.967	719
13	13-15-6-1	Hardlims-Hardlims	Purelin	0.510	2795
14	13-17-5-1	Satlins-Satlins	Purelin	0.928	1168

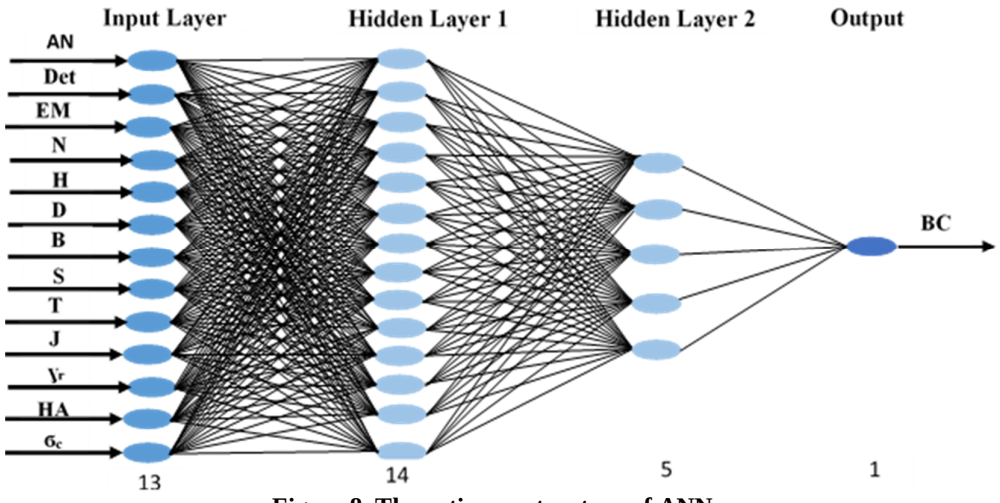

Figure 8. The optimum structure of ANNs.

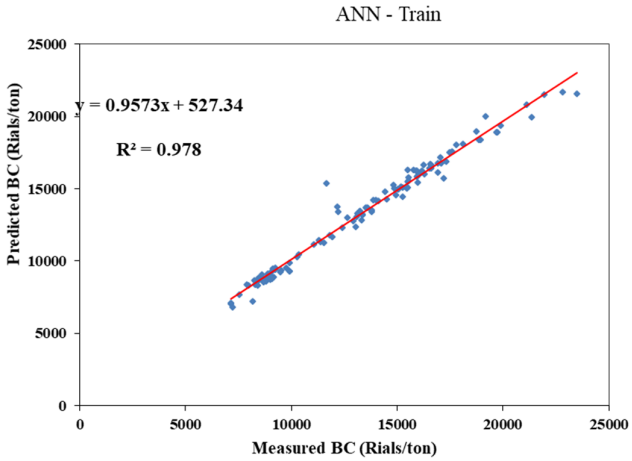

Figure 9. Relationship between the predicted and measured values of BC with the ANN model (in the train phase).

4.3. Prediction by multivariate regression

Multivariate regression is a statistical method used to explore the relationship between the dependent and independent variables and data analysis in modeling. It is also used to predict the dependent variable from the independent variables and obtain the relationship between them [52, 53]. Descriptive statistics for data adjustment and inferential statistics (correlation coefficient and multivariate regression) were used to predict BC after collecting the raw data.

In this method, 146 blasting records from six limestones of Iran were applied; 80% of the records were randomly used for modeling and 20% were used for the testing model. In the NLMR and LMR methods, the 13 parameters mentioned in Table 2 were used as the model inputs. The LMR model was created using the SPSS 24 software and forward method in order to predict BC [23]:

$$BC = 22148.722 - 6624.528S - 0.597AN + 217.96D - 1711.786T \quad (18)$$

In addition to the linear model, the data was processed by the non-linear polynomial, power, exponential, and logarithmic models. With respect to the higher R^2 value of the logarithmic model than the other non-linear models, it was used for BC prediction as follows:

$$BC = \frac{10^{5.648}}{S^{1.627} \times N^{0.28} \times H^{0.176}} \quad (19)$$

Figure 10 displays the relationship between the measured and predicted values of the BC values with the NLMR model in the train phase.

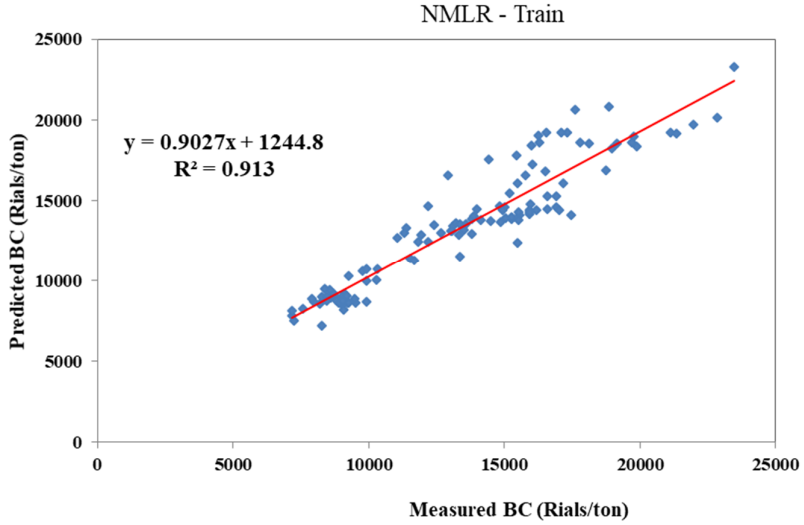

Figure 10. Relationship between the predicted and measured values of BC with the NMLR model (in train phase).

5. Discussion

We used 13 similar parameters as the inputs for modeling using the ANN, GEP, NLMR, and LMR methods in order to compare their results. The parameters were the ANFO value, number of detonators, Emolite value, hole number, hole length, hole diameter, burden, spacing, stemming, sub-drilling, specific gravity of rock, hardness, and uniaxial compressive strength.

In the present work, the basis of the performance evaluation of models was to compare the results with each other and with the actual data. The statistical indices of RMSE and R^2 were used for this purpose [38, 52, 53]. The performance evaluation indices were calculated for the proposed models according to the training and testing data (Table 7).

Table 7. Performance indices for the four models.

Model	Training stage		Testing stage	
	R^2	RMSE	R^2	RMSE
Linear multivariate regression	0.885	1210	0.855	1161
Nonlinear multivariate regression	0.913	1089	0.931	1098
Gene expression programming	0.943	961	0.933	1088
Artificial neural network	0.978	581	0.954	973

Theoretically, a prediction model is excellent when $R^2 = 1$ and RMSE = 0. The accuracy of the results of the GEP and ANN models compared to the actual values of BC in the testing phase is illustrated in Figures 11 and 12. Also the amount of consistency resulting from these models with the actual data is shown in Figures 13 and 14, respectively. As displayed in Table 7, the R^2 values were 0.855, 0.931, 0.933, and 0.954 for the LMR, NLMR, GEP, and ANN models, respectively, while the RMSE values for these four models were calculated as 1161, 1098, 1088, and 973, respectively, suggesting the superiority of the ANN model. As observed, the consistency and accuracy of the ANN model (with real data) are significantly higher than those of the LMR, NLMR, and GEP models. Although ANN is regarded as one of the intelligent and powerful techniques in parameter prediction, its most important drawback is the inability to provide a mathematical equation for engineering operations. On the other hand, based on the results given in Table 7, the GEP model showed a more reliable output by providing a mathematical equation to predict BC.

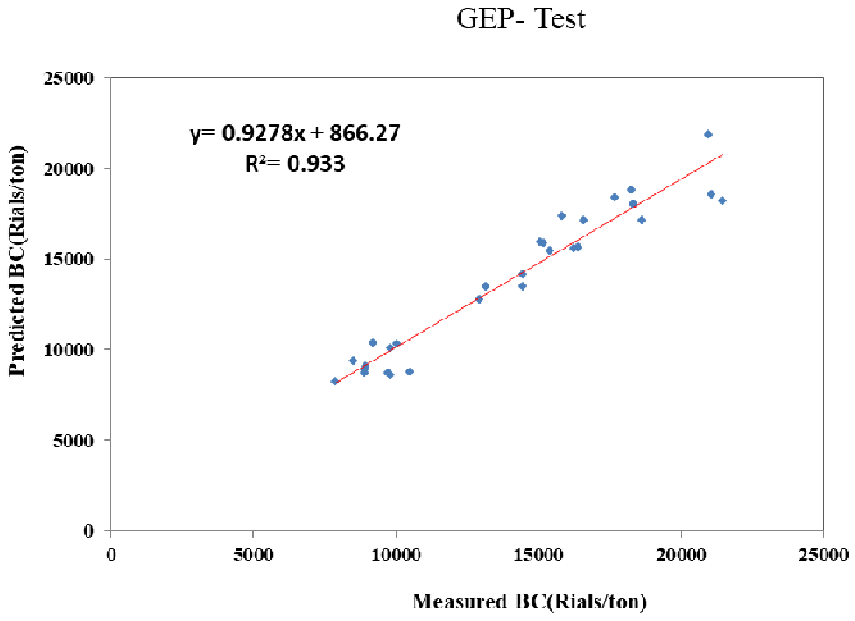

Figure 11. Relationship between the predicted and measured values of BC with the GEP model.

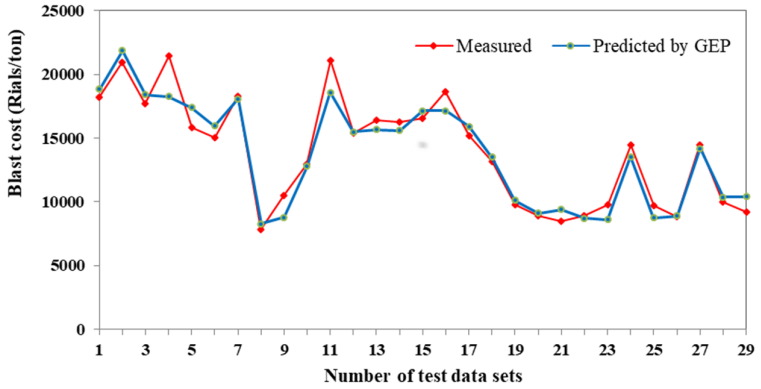

Figure 12. Relationship between the predicted and measured values of BC with the ANN model.

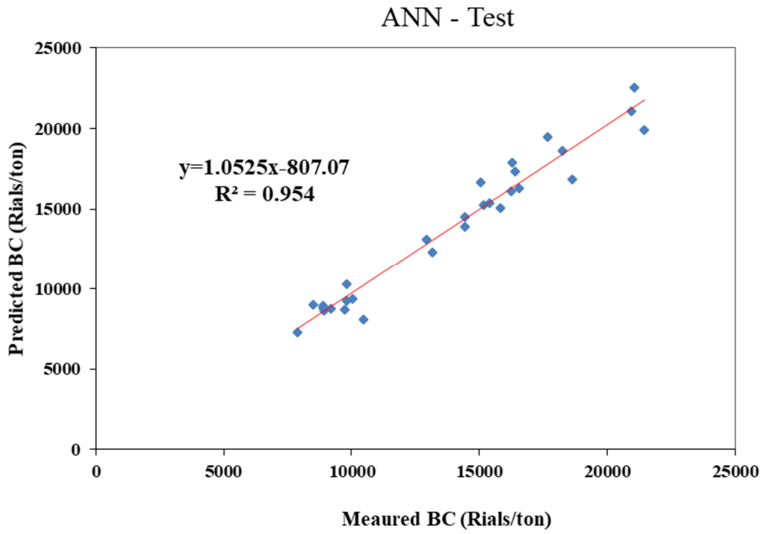

Figure 13. Comparison of the predicted cost of the GEP model with the actual cost in the testing phase.

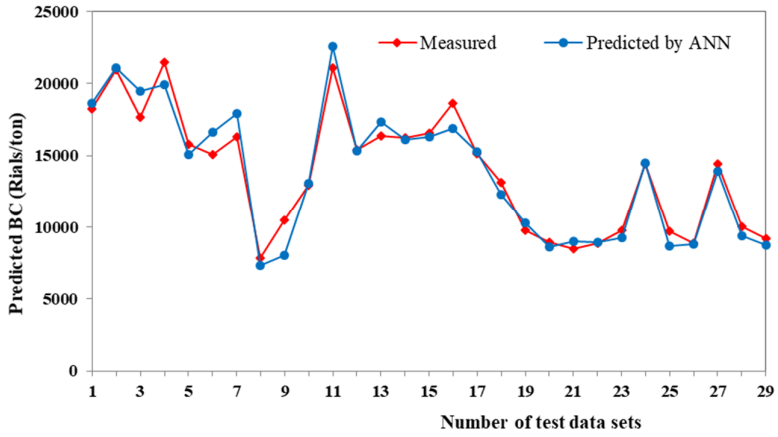

Figure 14. Comparison of the predicted cost of the ANN model with the actual cost in the testing phase.

6. Sensitivity analysis

One of the basic measures after modeling is to determine the sensitivity of the output parameter to each input parameter. In other words, the relative impact of the input parameters on the BC function can be determined by implementing the real values and the developed ANN model using the sensitivity analysis (Equation 20). For this purpose, the Relevancy Factor (RF) method was used in the present work [54, 55]:

$$r(p_k,\mu)=\frac{\sum_{i=1}^{n}(p_{k,i}-\bar{p}_k)\times(\mu_i-\bar{\mu})}{\sqrt{\sum_{i=1}^{n}(p_{k,i}-\bar{p}_k)^2\times\sum_{i=1}^{n}(\mu_i-\bar{\mu})^2}} \quad (20)$$

where $P_{k,i}$ indicates the ith value of the kth input parameter, $\bar{P}_k$ represents the average value related to the k^{th} parameter, μ_i means the ith value for the output parameter, $\bar{\mu}$ is considered as the average value for the output parameter, and n shows the number of input variables.

Figure 15 displays the results of the ANNs model sensitivity analysis using Equation 20. As shown, the spacing and ANFO values have the most and least effects on the BC function, respectively.

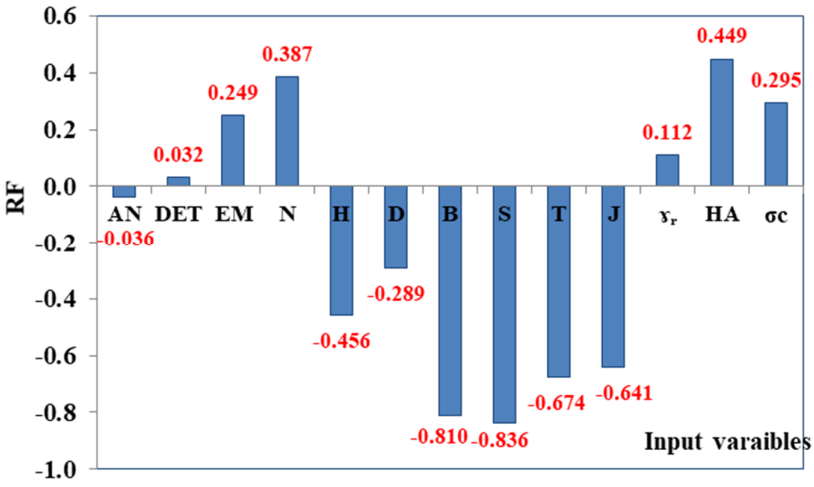

Figure 15. Sensitivity analysis of BC based on the input variables.

7. Conclusions

In the present work, the LMR, NLMR, GEP, and ANN models were used for BC prediction after collecting 146 datasets from six limestone mines in Iran and determining the input parameters and blasting constraints. The model presented with the ANN model in the testing step had a lower RMSE (973) and a higher R^2 (0.954) than the LMR, NLMR, and GEP models. Comparing the results of the ANN model with those of the LMR, NLMR, and GEP models based on the real data indicated that the ANN model was more consistent with the real BCs. The MLP network was used in two hidden layers with 14 and 5 neurons, and Logsig, Tansig, and purlin transfer functions, while the architecture 13-14-5-1 was used in the feed-forward back-propagation algorithm as the best combination for predicting BC. The RF method was used in ANNs for sensitivity analysis of the target function to the input parameters, and the results obtained indicated that the spacing and ANFO values had the highest and least effects on the BC function, respectively. In addition, a positive correlation was observed between the number of detonators, the amount of Emolite, hole number, specific gravity, hardness, and uniaxial compressive strength of rock and BC function, while a negative correlation was reported between the ANFO value, hole length, hole diameter, burden, spacing, stemming, sub-drilling, and BC function. Although this model can estimate BCs with a high reliability, some factors may lead to uncertainty in the model. Therefore, it is suggested that the proposed models be optimized and modified considering the uncertainty parameters.

Acknowledgments

We wish to thank the technical officer of Nurabad and Moslemabad mines as well as the chief of Tajareh, Abelou Neka, Tang Fani Poldokhtar, Sepahan Mobarakeh mines for their generous assistance in data collection and research.

References

[1]. Singh, T. and Singh, V. (2005). An intelligent approach to prediction and control ground vibration in mines. Geotech Geol Eng. 23 (3): 249-262.

[2]. Bhandari, S. (1997). Engineering rock blasting operations. Taylor & Francis, Boca Raton.

[3]. Singh, J., Verma, A., Banka, H., Singh, T. and Maheshwar, S. (2016). A study of soft computing models for prediction of longitudinal wave velocity. Arab J Geosci. 9 (3): 224.

[4]. Verma, A. and Singh, T. (2011). Intelligent systems for ground vibration measurement: a comparative study. Eng Comput. 27 (3): 225-233.

[5]. Jimeno, C.L., Jimeno, E.L. and Ayala Carcedo, F.J. (1995) Drilling and blasting of rocks. A.A Balkema, Rotterdam

[6]. Kanchibotla, S.S. (2003). Optimum blasting? Is it minimum cost per broken rock or maximum value per broken rock? Fragblast. 7 (1): 35-48.

[7]. Rajpot, M. (2009). The effect of fragmentation specification on blasting cost. Queen's university Kingston, Ontario, Canada.

[8]. Usman, T. and Muhammad, K. (2013). Modeling of blasting cost at Deewan Cement Quarry, Hattar using Multivariate Regression. J Eng And Appl Sci. 32 (1): 77-82.

[9]. Afum, B. and Temeng, V. (2015). Reducing Drill and Blast Cost through Blast Optimisation–A Case Study. Ghana Min J. 15 (2): 50-57.

[10]. Adebayo, B. and Mutandwa, B. (2015). Correlation of blast-hole deviation and area of block with fragment size and fragmentation cost. Int Res J Eng Tech. 2 (7): 402-406.

[11]. Ghanizadeh Zarghami, A., Shahriar, K., Goshtasbi, K. and Akbari, A. (2018). A model to calculate blasting costs using hole diameter, uniaxial compressive strength, and joint set orientation. J S Afr Inst Min Metall. 118 (8): 869-877.

[12]. Miranda, V., Leite, F. and Frank, G. (2019). A numerical approach blast pattern expansion. O-Pitblast Lda, Porto, Portugal.

[13]. Bakhshandeh Amnieh, H., Hakimiyan Bidgoli, M., Mokhtari, H. and Aghajani Bazzazi, A. (2019). Application of simulated annealing for optimization of blasting costs due to air overpressure constraints in open-pit mines. Journal of Mining and Environment(JME).

[14]. Singh, T. and Verma, A. (2010). Sensitivity of total charge and maximum charge per delay on ground vibration. Geomat Nat Haz Risk. 1 (3): 259-272.

[15]. Sharma, L., Singh, R., Umrao, R., Sharma, K. and Singh, T. (2017). Evaluating the modulus of elasticity of soil using soft computing system. Eng Comput. 33 (3): 497-507.

[16]. Faradonbeh, R.S., Armaghani, D.J. and Monjezi, M. (2016). Development of a new model for predicting flyrock distance in quarry blasting: a genetic programming technique. B Eng Geol Environ. 75 (3): 993-1006.

[17]. Álvarez-Vigil, A.E., González-Nicieza, C., López Gayarre, F. and Álvarez-Fernández, M.I. (2012). Predicting blasting propagation velocity and vibration frequency using artificial neural networks. Int J Rock Mech Min. 55: 108-116. doi:https://doi.org/10.1016/j.ijrmms.2012.05.002

[18]. Trivedi, R., Singh, T. and Raina, A. (2014). Prediction of blast-induced flyrock in Indian limestone mines using neural networks. J Rock Mech Geotech Eng. 6 (5): 447-454.

[19]. Nguyen, H., Bui, X.-N., Tran, Q.-H., Le, T.-Q. and Do, N.-H. (2019). Evaluating and predicting blast-induced ground vibration in open-cast mine using ANN: a case study in Vietnam. SN Applied Sciences. 1 (1): 125.

[20]. Çanakcı, H., Baykasoğlu, A. and Güllü, H. (2009). Prediction of compressive and tensile strength of Gaziantep basalts via neural networks and gene expression programming. J Neural Comput Appl. 18 (8): 1031-1041.

[21]. Ahangari, K., Moeinossadat, S.R. and Behnia, D. (2015). Estimation of tunnelling-induced settlement by modern intelligent methods. Soils Found. 55 (4): 737-748.

[22]. Monjezi, M., Baghestani, M., Faradonbeh, R.S., Saghand, M.P. and Armaghani, D.J. (2016). Modification and prediction of blast-induced ground vibrations based on both empirical and computational techniques. Eng Comput. 32 (4): 717-728.

[23]. Dehghani, H. (2018). Forecasting copper price using gene expression programming. Journal of Mining and Environment(JME). 9 (2): 349-360.

[24]. Ferreira, C. (2001). Gene expression programming: a new adaptive algorithm for solving problems. Complex Syst. 13 (2): 87-129.

[25]. Steeb, W.-H. (2014). The nonlinear workbook: Chaos, fractals, cellular automata, genetic algorithms, gene expression programming, support vector machine, wavelets, hidden Markov models, fuzzy logic with C++. World Scientific Publishing Company, Singapore.

[26]. Brownlee, J. (2011). Clever algorithms: nature-inspired programming recipes. Jason Brownlee, Melbourne,Australia.

[27]. Mollahasani, A., Alavi, A.H. and Gandomi, A.H. (2011). Empirical modeling of plate load test moduli of soil via gene expression programming. Comput Geotech. 38 (2): 281-286.

[28]. Yang, Y., Li, X., Gao, L. and Shao, X. (2013). A new approach for predicting and collaborative evaluating the cutting force in face milling based on gene expression programming. J Netw Comput Appl. 36 (6): 1540-1550.

[29]. Yassin, M.A., Alazba, A. and Mattar, M.A. (2016). Artificial neural networks versus gene expression programming for estimating reference evapotranspiration in arid climate. Agri Water Manage. 163: 110-124.

[30]. Ozbek, A., Unsal, M. and Dikec, A. (2013). Estimating uniaxial compressive strength of rocks using genetic expression programming. J Rock Mech Geotech Eng. 5 (4): 325-329.

[31]. Dindarloo, S.R. and Siami-Irdemoosa, E. (2016). Estimating the unconfined compressive strength of carbonate rocks using gene expression programming. Eur J Sci Res. 135 (3): 309-316.

[32]. Khandelwal, M., Armaghani, D.J., Faradonbeh, R.S., Ranjith, P. and Ghoraba, S. (2016). A new model based on gene expression programming to estimate air flow in a single rock joint. Environ Earth Sci. 75 (9): 1-13.

[33]. Faradonbeh, R.S. and Monjezi, M. (2017). Prediction and minimization of blast-induced ground vibration using two robust meta-heuristic algorithms. Eng Comput. 33 (4): 835-851.

[34]. Ferreira, C. (2006). Gene expression programming: mathematical modeling by an artificial intelligence,2nd. Springer, Germany.

[35]. Faradonbeh, R.S., Monjezi, M. and Armaghani, D.J. (2016). Genetic programing and non-linear multiple regression techniques to predict backbreak in blasting operation. Eng Comput. 32 (1): 123-133.

[36]. Teodorescu, L. and Sherwood, D. (2008). High energy physics event selection with gene expression programming. Comput Phys Commun. 178 (6): 409-419.

[37]. Güllü, H. (2012). Prediction of peak ground acceleration by genetic expression programming and regression: a comparison using likelihood-based measure. Eng Geol. 141: 92-113.

[38]. Armaghani, D.J., Faradonbeh, R.S., Momeni, E., Fahimifar, A. and Tahir, M. (2018). Performance prediction of tunnel boring machine through developing a gene expression programming equation. Eng Comput. 34 (1): 129-141.

[39]. Trippi, R.R. and Turban, E. (1992). Neural networks in finance and investing: Using artificial intelligence to improve real world performance. McGraw-Hill, Inc., New York.

[40]. Monjezi, M., Ahmadi, M., Sheikhan, M., Bahrami, A. and Salimi, A. (2010). Predicting blast-induced ground vibration using various types of neural networks. Soil Dynamics and Earthquake Engineering. 30 (11): 1233-1236.

[41]. Nguyen, H., Bui, X.-N., Bui, H.-B. and Mai, N.-L. (2018). A comparative study of artificial neural networks in predicting blast-induced air-blast overpressure at Deo Nai open-pit coal mine, Vietnam. J Neural Comput Appl: 1-17.

[42]. Anderson, J.A. (1995). An introduction to neural networks. MIT press.

[43]. Chauvin, Y. and Rumelhart, D.E. (2013). Backpropagation: theory, architectures, and applications. Psychology Press.

[44]. Neaupane, K.M. and Achet, S.H. (2004). Use of backpropagation neural network for landslide monitoring: a case study in the higher Himalaya. Eng Geol. 74 (3-4): 213-226.

[45]. Wasserman, P.D. (1993). Advanced methods in neural computing. John Wiley & Sons, Inc.

[46]. Mehrdanesh, A., Monjezi, M. and Sayadi, A.R. (2018). Evaluation of effect of rock mass properties on fragmentation using robust techniques. Eng Comput. 34 (2): 253-260.

[47]. Bakhsandeh Amnieh, H., Mohammadi, A. and Mozdianfard, M. (2013). Predicting peak particle velocity by artificial neural networks and multivariate regression analysis-Sarcheshmeh copper mine, Kerman, Iran. Journal of Mining and Environment(JME). 4 (2): 125-132.

[48]. Monjezi, M., Mehrdanesh, A., Malek, A. and Khandelwal, M. (2013). Evaluation of effect of blast design parameters on flyrock using artificial neural networks. J Neural Comput Appl. 23 (2): 349-356.

[49]. Faradonbeh, R.S., Armaghani, D.J., Majid, M.A., Tahir, M.M., Murlidhar, B.R., Monjezi, M. and Wong, H. (2016). Prediction of ground vibration due to quarry blasting based on gene expression programming: a new model for peak particle velocity prediction. Int J Environ Sci Technol. 13 (6): 1453-1464.

[50]. Keshavarz, A. and Mehramiri, M. (2015). New Gene Expression Programming models for normalized shear modulus and damping ratio of sands. Eng Appl Artif Intel. 45: 464-472.

[51]. Moshrefi, S., Shahriar, K., Ramezanzadeh, A. and Goshtasbi, K. (2018). Prediction of ultimate strength of shale using artificial neural network. Journal of Mining and Environment(JME). 9 (1): 91-105.

[52]. Majdi, A. and Rezaei, M. (2013). Prediction of unconfined compressive strength of rock surrounding a roadway using artificial neural network. J Neural Comput Appl. 23 (2): 381-389.

[53]. Rezaei, M., Majdi, A. and Monjezi, M. (2014). An intelligent approach to predict unconfined compressive strength of rock surrounding access tunnels in longwall coal mining. J Neural Comput Appl. 24 (1): 233-241.

[54]. Saltelli, A., Ratto, M., Andres, T., Campolongo, F., Cariboni, J., Gatelli, D., Saisana, M. and Tarantola, S. (2008). Global sensitivity analysis: the primer. John Wiley & Sons.

[55]. Sebastian, H., Wenger, R. and Renner, T. (1985). Correlation of minimum miscibility pressure for impure CO2 streams. J Pet Technol. 37 (11): 2076-2082.

Appendix 1

Table A-1. Datasets used for constructing models.

Case No.	Input parameters													Constraints			Output
	AN	Det	EM	N	H	D	B	S	T	J	γr	HA	σc	Fr	FL	BB	BC
1	5,500	270	260	270	6.3	76	1.8	2.1	0.9	0.5	2.7	3.5	671	25	140	3	18,239
2	9,300	490	500	436	6.8	76	1.8	2.2	0.9	0.5	2.7	3.5	671	27	140	3	15,486
3	10,000	650	500	404	8	76	1.7	2	0.9	0.5	2.7	3.5	671	25	140	3.5	18,110
4	4,300	230	280	215	6	76	1.7	2	1	0.5	2.7	3.5	671	25	120	4	23,481
5	6,200	590	320	500	4	76	1.8	2	1.1	0.5	2.7	3.5	671	30	120	4	20,946
6	10,000	500	600	350	9	76	1.7	2	1	0.5	2.7	3.5	671	25	120	4.3	19,753
7	10,000	553	480	553	5.4	76	1.7	2	1	0.5	2.7	3.5	671	25	120	4	18,948
8	5,300	350	280	348	4.7	76	2	2.5	1.2	0.6	2.7	3.5	671	40	100	5	15,959
9	6,600	480	400	480	4.4	76	1.8	2.2	1.1	0.5	2.7	3.5	671	30	100	4	18,738
10	6,500	350	380	350	6	76	1.8	2.1	1.1	0.5	2.7	3.5	671	30	120	4	17,684
11	7,300	400	360	400	5.3	76	1.7	2.1	1	0.5	2.7	3.5	671	26	120	4	19,165
12	6,500	500	360	500	4	76	1.7	2	1	0.5	2.7	3.5	671	25	110	4	21,949
13	10,000	470	580	470	6.3	76	1.7	2	1	0.5	2.7	3.5	671	25	115	4.5	19,705
14	10,000	440	520	399	7	76	1.7	2	1	0.5	2.7	3.5	671	25	110	4	21,449
15	8,500	480	400	480	5	76	1.7	2	1	0.5	2.7	3.5	671	27	110	4	21,131
16	10,000	440	440	387	7.2	76	1.7	2	1	0.5	2.7	3.5	671	25	112	4	21,345
17	6,700	500	340	468	4	76	1.7	2	1	0.5	2.7	3.5	671	25	110	4	22,837
18	8,200	500	440	498	4.8	76	1.9	2.3	1.1	0.6	2.7	3.5	671	35	100	5	16,918
19	8,600	500	500	500	5.2	76	2	2.2	1.2	0.6	2.7	3.5	671	40	100	5	15,804
20	9,500	500	460	500	5.4	76	1.9	2.2	1.1	0.6	2.7	3.5	671	35	105	5.5	17,182
21	7,800	440	360	422	5	76	1.8	2.1	1.1	0.5	2.7	3.5	671	30	100	5	19,897
22	10,000	500	500	500	6	76	1.8	2.3	1.1	0.5	2.7	3.5	671	30	100	5	15,009
23	9,700	500	480	495	6.2	76	1.8	2.3	1.1	0.5	2.7	3.5	671	30	100	5	14,828
24	9,200	400	400	394	6.9	76	1.8	2.3	1.1	0.5	2.7	3.5	671	30	100	5	16,592
25	7,900	400	380	355	7.7	76	1.8	2.3	1.1	0.5	2.7	3.5	671	30	100	5	15,049
26	10,000	460	460	445	7	76	2	2.5	1.2	0.6	2.7	3.5	671	40	100	5	13,315
27	6,800	280	300	281	7.6	76	2	2.5	1.2	0.6	2.7	3.5	671	40	105	5	13,983
28	8,800	430	380	430	6.5	76	2	2.5	1.2	0.6	2.7	3.5	671	40	100	5	13,504
29	8,100	430	380	429	5.8	76	2	2.2	1.2	0.6	2.7	3.5	671	40	100	5	15,763
30	8,400	370	320	362	7	76	1.9	2.2	1.1	0.6	2.7	3.5	671	35	110	4	16,514
31	10,000	500	460	391	8.2	76	1.9	2.1	1.1	0.6	2.7	3.5	671	35	110	5	16,036
32	8000	440	300	440	5.7	76	1.9	2.1	1.7	0.6	2.7	3.5	671	40	140	3	16,283
33	3200	200	120	194	5.4	76	2.7	3.2	1.4	0.5	2.6	3	530	25	140	3	11,546
34	3100	200	70	80	11	76	2.7	3.2	2.0	0.5	2.6	3	530	35	80	4	13,796
35	7000	320	180	230	8.7	76	2.7	3.2	1.7	0.5	2.6	3	530	30	110	4	9,932
36	6000	220	200	220	8	76	2.7	3.2	1.6	0.5	2.6	3	530	30	120	4	9,261
37	7700	340	180	310	7.5	76	2.7	3.2	1.5	0.5	2.6	3	530	25	130	3	8,552
38	9800	360	220	360	8	76	2.7	3.2	1.6	0.5	2.6	3	530	30	120	4	7,868
39	11400	520	300	520	6.8	76	2.8	3.4	1.5	0.6	2.6	3	530	35	130	5	7,233
40	9650	520	240	460	6.6	76	2.8	3.4	1.4	0.6	2.6	3	530	35	140	5	7,164
41	7900	420	180	380	6.5	76	2.8	3.4	1.4	0.6	2.6	3	530	35	140	5	7,559
42	9100	380	200	380	7.3	76	2.8	3.4	1.6	0.6	2.6	3	530	40	110	5	7,157
43	9050	240	140	210	8.5	76	2.8	3.4	1.8	0.6	2.6	3	530	35	90	5	10,466
44	9050	520	200	260	10	76	2.8	3.4	1.9	0.6	2.6	3	530	40	85	6	8,189
45	10250	370	300	270	12	76	2	3	2	0.5	2.65	3.2	550	35	80	4.5	10,278
46	9860	380	460	300	10.3	76	2	2.5	1.8	0.5	2.65	3.2	550	35	85	5	13,109
47	9000	460	440	460	6.7	76	2	2.5	1.7	0.5	2.65	3.2	550	35	100	5	11,934
48	10000	460	300	330	9.7	76	2	2.5	1.8	0.5	2.65	3.2	550	35	85	5	12,915
49	8800	510	350	510	6.2	76	2	2.5	1.7	0.5	2.65	3.2	550	35	100	5	11,064

Table A-1. Datasets used for constructing models.

50	9860	460	300	230	13	76	2	2.5	2	0.5	2.65	3.2	550	35	80	5	13,783
51	9800	310	285	310	10.2	76	1.8	2	2	0.5	2.65	3.2	550	25	80	4	16,555
52	10500	300	210	157	13	96	2.4	3	2	0.6	2.65	3.2	550	45	110	6	13,356
53	9200	347	320	347	8.6	76	1.8	1.9	1.7	0.5	2.65	3.2	550	25	120	3	18,862
54	9350	400	270	396	7.4	76	1.8	1.9	1.3	0.5	2.65	3.2	550	25	140	3	17,612
55	5900	250	180	128	9	96	2.3	2.4	1.6	0.6	2.65	3.2	550	40	120	4	21,060
56	12400	320	250	190	12.4	96	2.3	2.6	1.8	0.6	2.65	3.2	550	40	120	5	15,250
57	10660	280	230	170	12	96	2.3	2.6	1.8	0.6	2.65	3.2	550	40	120	5	16,187
58	10700	290	230	200	10.5	96	2.3	2.6	1.8	0.6	2.65	3.2	550	40	120	5	15,549
59	10800	330	220	190	11	96	2.3	2.6	1.8	0.6	2.65	3.2	550	40	120	5	15,913
60	11100	270	240	210	10.3	96	2.3	2.6	1.7	0.6	2.65	3.2	550	40	120	5	15,049
61	10800	270	240	210	10	96	2.3	2.6	1.7	0.6	2.65	3.2	550	40	120	5	15,408
62	10500	290	220	160	12.3	96	2.3	2.6	1.6	0.6	2.65	3.2	550	40	130	4	16,919
63	10700	300	276	240	8.8	96	2.3	2.6	1.6	0.6	2.65	3.2	550	40	130	4	15,506
64	11350	300	230	200	11	96	2.3	2.6	1.7	0.6	2.65	3.2	550	43	110	4.5	15,248
65	11000	300	220	160	13.2	96	2.3	2.6	2.0	0.6	2.65	3.2	550	45	90	5	15,939
66	10250	310	250	180	11.2	96	2.3	2.6	1.9	0.6	2.65	3.2	550	45	100	5.5	16,380
67	11100	410	260	190	11.4	96	2.3	2.6	1.9	0.6	2.65	3.2	550	45	100	6	17,463
68	10700	300	250	160	13	96	2.3	2.6	2	0.6	2.65	3.2	550	47	90	6	16,590
69	11300	340	250	162	13.6	96	2.3	2.6	2.2	0.6	2.65	3.2	550	47	90	6	15,916
70	10260	310	230	170	11.8	96	2.3	2.6	2	0.6	2.65	3.2	550	47	90	6	17,030
71	11240	320	250	161	13.5	96	2.3	2.6	2.1	0.6	2.65	3.2	550	47	90	6	16,235
72	11300	270	260	162	13.5	96	2.3	2.6	2.1	0.6	2.65	3.2	550	47	90	6	15,527
73	11500	260	210	150	14.7	96	2.3	2.6	2.2	0.6	2.65	3.2	550	47	90	6	14,952
74	10000	390	268	390	8.5	76	1.7	2	1.5	0.2	2.63	3.3	600	30	80	1.5	16,292
75	9700	340	270	333	9	76	1.7	2	1.6	0.3	2.63	3.3	600	35	60	1.5	17,306
76	9800	490	320	490	6.4	76	1.7	2	1.0	0.2	2.63	3.3	600	20	100	2	16,557
77	10000	330	290	324	10	76	1.7	2	1.6	0.3	2.63	3.3	600	30	80	1.5	16,244
78	9800	320	270	320	9.5	76	1.7	2	1.5	0.3	2.63	3.3	600	30	80	1.5	17,081
79	9900	400	350	242	10.5	90	2.6	3	2.6	0.5	2.63	3.3	600	38	80	1	9,764
80	9700	520	380	520	6.2	76	1.7	2	1.4	0.2	2.63	3.3	600	20	100	2	18,616
81	9800	440	380	398	8.2	76	1.7	2	1.5	0.3	2.63	3.3	600	35	70	2	17,799
82	9900	450	180	447	7.2	76	1.7	2	1.5	0.3	2.63	3.3	600	25	90	2	15,987
83	9700	320	340	240	10	90	2.6	3	2.6	0.4	2.63	3.3	600	38	80	1	9,924
84	10000	520	340	480	7	76	1.8	2.1	1.1	0.2	2.63	3.3	600	25	90	2	15,164
85	9800	360	300	350	9	76	1.8	2.1	1.5	0.2	2.63	3.3	600	40	60	1.5	14,421
86	8700	530	400	300	10	76	2	2.5	2	1	2.7	3.3	620	30	90	1.8	13,591
87	8400	400	380	320	8.8	76	2	2.5	2	1	2.7	3.3	620	30	90	1.8	13,232
88	9500	380	360	380	8.2	76	2	2.5	2	1	2.7	3.3	620	30	90	1.8	13,030
89	8300	500	320	290	9.8	76	2	2.5	2	1	2.7	3.3	620	30	90	1.8	13,141
90	8700	400	380	310	9.7	76	2	2.5	2	1	2.7	3.3	620	30	90	1.8	12,393
91	9800	420	420	360	9	76	2	2.5	2	1	2.7	3.3	620	30	90	1.8	13,079
92	8500	400	360	320	9.8	76	2	2.5	2	1	2.7	3.3	620	30	90	1.8	11,370
93	9700	390	320	385	8.3	76	2	2.5	2	1	2.7	3.3	620	30	90	1.8	11,316
94	6900	220	200	155	10	90	3	3.5	2.5	1.5	2.7	3.3	620	45	75	3	9,795
95	10000	260	240	195	9.2	100	3.5	4	2.1	1.5	2.7	3.3	620	45	80	3	8,271
96	7800	200	160	170	10	90	3	3.5	2.5	1.5	2.7	3.3	620	45	75	3	9,118
97	10000	260	230	130	17	90	3	3.5	2.5	1.5	2.7	3.3	620	45	75	3	8,282
98	10000	260	270	133	15.8	90	3	3.5	2.5	1.5	2.7	3.3	620	45	75	3	8,912
99	10000	270	320	135	16	90	3	3.5	2.5	1.5	2.7	3.3	620	45	75	3	9,058
100	10000	280	380	134	16.7	90	3	3.5	2.5	1.5	2.7	3.3	620	45	75	3	8,618
101	10000	280	300	129	17	90	3	3.5	2.5	1.5	2.7	3.3	620	45	75	3	8,664
102	10000	290	270	136	16.1	90	3	3.5	2.5	1.5	2.7	3.3	620	45	75	3	9,021

Table A-1. Datasets used for constructing models.

103	8500	250	260	125	16	90	3	3.5	2.5	1.5	2.7	3.3	620	45	75	3	8,512
104	10000	270	330	132	16.3	90	3	3.5	2.5	1.5	2.7	3.3	620	45	75	3	9,174
105	9800	280	280	130	16.5	90	3	3.5	2.5	1.5	2.7	3.3	620	45	75	3	8,696
106	10000	300	300	127	17.7	90	3	3.5	2.5	1.5	2.7	3.3	620	45	75	3	8,461
107	10000	400	300	200	11	90	3	3.5	2.5	1.5	2.7	3.3	620	45	75	3	9,532
108	10000	330	290	162	13.6	90	3	3.5	2.5	1.5	2.7	3.3	620	45	75	3	8,887
109	10000	400	270	200	11	90	3	3.5	2.5	1.5	2.7	3.3	620	45	75	3	9,223
110	10000	380	280	190	11.3	90	3	3.5	2.5	1.5	2.7	3.3	620	45	75	3	9,903
111	9000	300	340	199	10.8	90	3	3.5	2.5	1.5	2.7	3.3	620	45	75	3	8,883
112	9500	100	430	190	11.6	90	3	3.5	2.5	1.5	2.7	3.3	620	45	75	3	7,971
113	10000	400	320	210	10.7	90	3	3.5	2.5	1.5	2.7	3.3	620	45	75	3	9,792
114	10000	430	350	215	10.6	90	3	3.5	2.5	1.5	2.7	3.3	620	45	75	3	9,046
115	9800	400	310	200	11.0	90	3	3.5	2.5	1.5	2.7	3.3	620	45	75	3	9,261
116	8200	310	320	310	7.6	76	2	2.5	1.7	1	2.7	3.3	620	25	100	1.5	13,882
117	8900	350	400	315	8.3	76	2	2.5	1.7	1	2.7	3.3	620	25	100	1.5	14,127
118	9200	510	440	320	8.6	76	2	2.5	1.7	1	2.7	3.3	620	25	100	1.5	14,425
119	9200	570	460	325	8.3	76	2	2.5	1.6	1	2.7	3.3	620	25	100	1.5	14,877
120	9400	450	380	330	8.5	76	2	2.5	1.7	1	2.7	3.3	620	25	100	1.5	13,365
121	9500	400	440	316	7.2	90	3	3.5	2	1.5	2.7	3.3	620	38	80	2	9,072
122	8600	346	360	346	7.2	76	2	2.5	2	1	2.7	3.3	620	30	90	1.8	14,495
123	9900	270	300	162	14	90	3	3.5	2.5	1.5	2.7	3.3	620	45	75	3	8,442
124	10000	280	360	170	12.6	90	3	3.5	2.5	1.5	2.7	3.3	620	45	75	3	9,721
125	9800	330	230	165	13.2	90	3	3.5	2.5	1.5	2.7	3.3	620	45	75	3	8,887
126	10000	260	360	175	12.6	90	3	3.5	2.5	1.5	2.7	3.3	620	45	75	3	8,829
127	10000	330	270	108	20.4	90	3	3.5	3.6	1.5	2.7	3.3	620	45	75	3	8,708
128	9400	330	240	165	12.6	90	3	3.5	2.5	1.5	2.7	3.3	620	45	75	3	9,466
129	9800	290	320	243	9	90	3	3.5	2.5	1.5	2.7	3.3	620	45	75	3	8,876
130	9800	420	370	420	7.4	76	2	2.5	2	1	2.7	3.3	620	30	90	1.7	12,660
131	9800	320	290	201	10.8	90	3	3.5	2.5	1.5	2.7	3.3	620	45	80	3	8,936
132	10000	340	350	168	13	90	3	3.5	2.5	1.5	2.7	3.3	620	45	80	3	9,038
133	1470	112	40	56	9	76	2.4	3	2.2	1	2.6	3	540	30	100	1.3	14,435
134	3700	172	150	86	10.4	90	3.5	4	2.5	1	2.6	3	540	45	90	2	7,911
135	2600	120	120	60	10	90	3.3	3.8	2.3	1	2.6	3	540	40	90	2	10,337
136	2070	157	80	87	8.4	76	2.4	3	2	0.8	2.6	3	540	30	110	1.1	12,195
137	2800	90	100	80	8	90	3.5	4	2.2	1.1	2.6	3	540	45	90	2	8,396
138	1650	78	60	38	10.4	90	3.5	4	2.5	1.1	2.6	3	540	45	90	2	10,024
139	1380	108	40	54	9	76	2.4	3.8	2.2	0.9	2.6	3	540	30	100	1.2	11,669
140	1620	78	60	38	10.4	90	3	3	2.5	1.1	2.6	3	540	40	90	1.5	15,448
141	1500	70	60	35	10.4	76	2.4	3.8	2	1	2.6	3	540	30	110	1.1	15,503
142	3670	180	140	90	10	90	3.2	3.8	2.5	1.1	2.6	3	540	45	85	2	9,181
143	2340	112	80	56	10.4	90	3	3.5	2.5	1.2	2.6	3	540	40	85	1.8	11,818
144	1020	73	40	73	5.5	76	2.4	3	1.5	0.5	2.6	3	540	20	110	1	12,930
145	2320	122	90	61	9	90	3	3.5	2.5	1	2.6	3	540	40	90	1.8	12,181
146	1020	45	40	29	8.5	90	3	3.5	2.5	1	2.6	3	540	40	90	1.8	15,182

In this Table, rows 1 to 32 belong to Tajareh Mine of Khorramabad, rows 33 to 44 belong to Tang Fani Mine of Pol Dokhtar, rows 45 to 73 belong to Barkhordar1 Mine of Nurabad, rows 74 to 85 belong to Moslem Abad Mine of Hamedan, rows 86 to 132 belong to Sepahan Mobarakeh Mine of Esfahan, and rows 133 to 146 belong to Abelou mine of Neka.

پیش بینی هزینه انفجار در معادن سنگ آهک با استفاده از مدل برنامه ریزی بیان ژن و شبکه عصبی مصنوعی

رضا بستامی[1]، عباس آقاجانی بزازی[2]، هادی حمیدیان شورمستی[3*]، کاوه آهنگری[1]

1- گروه مهندسی معدن، دانشگاه آزاد اسلامی، واحد علوم و تحقیقات، تهران، ایران
2- گروه مهندسی معدن، دانشگاه کاشان،کاشان، ایران
3- گروه مهندسی معدن، دانشگاه آزاد اسلامی واحد قائم‌شهر، قائم‌شهر، ایران

ارسال 2019/10/13، پذیرش 2019/12/29

* نویسنده مسئول مکاتبات: hhamidian@Qaemiau.ac.ir

چکیده:

پیش‌بینی هزینه انفجار برای ر سیدن به خردایش مطلوب با در نظر دا شتن کنترل پیامدهای نامطلوب نا شی از انفجارمانند پرتاب سنگ، لرزش زمین، انفجار هوا، درمعادن امری ضروری و قابل توجه است. در این پژوهش با جمع‌آوری 146داده انفجار از 6 معدن سنگ آهک در ایران با استفاده از مدل‌های شبکه عصبی مصنوعی (ANN)، برنامه‌ریزی بیان ژن (GEP)، رگرسیون چند متغیره خطی(LMR) و غیرخطی(NLMR) به پیش‌بینی هزینه انفجار پرداخته شد. درتمامی مدل ها از مقدارآنفو، تعدادچاشنی، مقدار امولایت، تعداد چال، طول چال، قطر چال، بار سنگ، فاصله‌داری، گل‌گذاری، اضافه‌حفاری، وزن مخصوص سنگ، سختی و مقاومت فشاری تک محوری به عنوان پارامترهای ورودی استفاده شد. مدل ANN در مرحله تست در مقایسه با سایرمدل‌ها ضریب همبستگی بیشتر (0/954) و جذر متو سط مربعات خطا کمتری (973) از خود ن شان داد. این مدل در مقای سه با سه مدل دیگر تطابق بهتری با هزینه‌های واقعی انفجار دا شت. اگرچه روش شبکه عصبی مصنوعی به عنوان یکی از تکنیک‌های هوشمند وقدرتمند درپیش‌بینی پارامترها به شمار می‌رود اما مهم ترین ایراد آن عدم امکان ارائه معادله ریاضی برای عملیات مهندسی است. درمقابل مدل GEP با ارائه یک معادله ریاضی پیش‌بینی هزینه انفجار، با ضریب همبستگی 0/933 و جذر متوسط مربعات خطا 1088 خروجی قابل اعتمادی را به نمایش گذاشت. براساس آنالیز حساسیت انجام گرفته فاصله‌داری بین چال‌ها و مقدار آنفو به‌ترتیب بیشترین و کمترین تأثیر را بر روی تابع هزینه انفجار دا شتند. تعدادچا شنی، مقدارامولایت، تعدادچال، وزن مخصوص، سختی ومقاومت فشاری تک محوری سنگ پارامترهایی هستند که با تابع هزینه انفجار همبستگی مثبت و میزان آنفو، طول چال، قطر چال، بارسنگ، فاصله‌داری ،گل‌گذاری، اضافه حفاری با تابع هزینه انفجار همبستگی منفی داشتند.

کلمات کلیدی: هزینه انفجار، معادن سنگ آهک، برنامه‌ریزی بیان ژن، رگرسیون چندمتغیره غیر خطی، شبکه عصبی مصنوعی، مدل سازی.